

RESEARCH ARTICLE

Observer-based Hybrid Event-triggered Model Predictive Tracking Control for Mecanum-wheeled Mobile Robot

Binghao Yang¹ | Dongliang Wang¹ | Ziling Wen¹ | Wu Wei² | Wenji Li¹ | Zhun Fan³

¹School of Department of Electronic and Information Engineering, Shantou University, Guangdong, China

²School of Automation Science and Engineering, South China University of Technology, Guangdong, China

³Shenzhen Institute for Advanced Study, University of Electronic Science and Technology of China, Guangdong, China

Correspondence

Corresponding author Dongliang Wang.
This is sample corresponding address.
Email: dlwang@stu.edu.cn

Funding Information

This research was supported by the Science and Technology Planning Project of Guangdong Province, China, Grant/Award Number: 2022A1515110566, 2023A1515011574, 2019A050520001); STU Scientific Research Initiation Grant NTF21052.

Abstract

With the increasing prevalence of omnidirectional mobile robots in industrial applications, such as collaborative transportation and cargo classification, the demand for computational power in these robots has grown significantly. Model Predictive Control (MPC) is widely used for trajectory tracking due to its exceptional ability to handle constraints; however, it is computationally intensive. Therefore, our core approach proposes a hybrid event-triggering mechanism to minimize the reliance on MPC. When the tracking error remains within a specified threshold, the system continues using the existing optimal control sequence without resolving the MPC optimization problem, thereby reducing computational complexity. However, less frequent use of MPC can lead to decreased tracking accuracy. To address this issue, we incorporate a novel sliding mode observer to compensate for errors and mitigate the effects of unknown disturbances. To validate the performance of the proposed controller, we conducted simulations comparing the trajectory tracking performance of traditional MPC, event-triggered MPC, and observer-based MPC under disturbance conditions. The results demonstrate that the proposed algorithm maintains tracking accuracy while significantly reducing computational load.

KEYWORDS:

mecanum-wheeled mobile robot, model predictive control, event-triggered control, sliding mode observer, trajectory tracking

1 | INTRODUCTION

As an omnidirectional mobile robot, the Mecanum-wheeled mobile robot (MWMR), with its superior motion capabilities and stability, finds increasing application across various domains^{1,2}. With the advancement of technology, the demands associated with MWMR's tasks are also on the rise. Notably, trajectory tracking stands out as a prominent research focus in the field of robotics and represents a pivotal technology for enabling MWMR to autonomously fulfill tasks^{3,4}. In order to achieve tracking control, scholars have proposed models such as the kinematics trajectory tracking error model⁵ and dynamic model⁶ for MWMR, etc. Given that MWMR is a nonlinear system with complicated constraints, the achievement of precise trajectory tracking proves challenging⁷.

To overcome these control difficulties, the exceptional capability of model predictive control (MPC) in effectively managing complex constraints, encompassing state, input and output in trajectory tracking problems, has garnered increasing favor among scholars^{8,9,10}. In¹¹, a novel distributed model predictive control has been proposed to achieve formation control of a team

consisting of four mobile robots. The authors of¹² proposed a novel MPC approach based on the dynamics of cooperative longitudinal motion of the vehicle platoon for addressing the issue of vehicle platoon control. To tackle the optimal coordination problem, an optimal hierarchical control framework with linear time-varying model predictive controller was developed in¹³. Another notable exploration¹⁴ introduced a reinforcement learning-based model predictive control, achieving trajectory tracking of unmanned surface vehicle. In¹⁵, a novel dual-loop nonlinear tube-based robust model predictive control algorithm was proposed, which ensured the actual system trajectories remained within a designated tube region centered around the nominal solution.

For trajectory tracking control of mobile robots, dynamic model provides better control effect than considering only kinematic model¹⁶. However, it is imperative to acknowledge that the computational complexity of MPC escalates with the QP problem dimension^{17,18}. This implies that MPC not only imposes a higher computational burden but also necessitates increased communication resources. In this regard, the event-triggering mechanism can effectively reduce the computation and communication cost^{19,20}. In one study²¹, to decrease the consumption of resources, a novel dynamic event-triggered mechanism was proposed by introducing a bounded dynamic variable and a time-varying threshold. In a separate study²², an event-triggered MPC was implemented for the control of autonomous vehicles path tracking within the CARLA simulation environment, aiming to decrease computation load. In²³, a quasi-differential type event-triggering mechanism was proposed, which reduced the number of event triggers by the event-triggering condition constructed by the error gradient. It is noteworthy that when the event is not triggered, the system will still employing the control sequence derived from the most recent MPC trigger. However, the dynamics model of MWMR is time-varying, implying that the system may experience a decrease in control accuracy due to model uncertainties²⁴. In addition, the external disturbances are also one of the reasons for the system errors²⁵. The presence of the aforementioned lumped disturbance results in high-frequency triggering of the controller²⁶, which contradicts our intended control strategy.

This issue has been studied in detail by many scholars, and various effective solutions have emerged. In²⁷, a statistical learning method was applied to event-triggered MPC to compensate for unknown disturbance. Similarly, an event-triggered extended state observer based robust MPC was proposed in²⁸, in which the observer was introduced to estimate the disturbances within the power converter systems. Li *et al.*²⁹ proposed a central path-based disturbance prediction approach to improve the state prediction precision and, hence, reduce greatly the triggering frequency. In³⁰, Liu *et al* presented a virtual stabilizing function aimed at eliminating the influence of the model uncertainties. The sliding mode observer, recognized as an effective method for disturbance estimation, has been extensively studied by scholars in recent years. To enhance the anti-disturbance capabilities of permanent magnet synchronous motor, based on the improved non-singular fast terminal sliding mode controller proposed in³¹, SMO was introduced to estimate the load disturbance. In³², a composite SMO was proposed for eliminating the effect of mismatch between inductance, resistance and magnetic chain parameters in motor systems. In³³, a fuzzy second-order SMO algorithm was employed in closed-loop control, successfully achieving trajectory tracking control of a two-link robot. Building upon the aforementioned discoveries, SMO is incorporated in this paper to mitigate perturbations within the control process.

Therefore, this paper proposes a SMO-based hybrid event-triggered model predictive control (SMO-HETMPC) for trajectory tracking of MWMR. Initially, for the trajectory tracking problem of MWMR, a hybrid triggering mechanism combining two triggering conditions is designed. The proposed triggering condition deviates from the traditional event-triggered MPC, which relies on the error between the actual state sequence and the optimal predicted state sequence for triggering. Instead, it utilizes the error state between the actual state sequence and the desired target sequence as the triggering condition, ensuring a certain level of path tracking accuracy. On this basis, this approach significantly reduces the computational load when compared to time-driven MPC. Meanwhile, to further reduce the trigger frequency, a SMO is introduced to compensate the control inputs, aiming to alleviate the impact of model errors and external disturbances. Specifically, a novel reaching law is designed in this paper. Finally, through experimental comparisons, the effectiveness and robustness of the proposed SMO-HETMPC are validated. In this paper, the major contributions are summarized as follows:

1. This paper proposes a novel hybrid event-triggering mechanism and demonstrates its effectiveness in mitigating Zeno behavior. Furthermore, experimental results confirm that the proposed mechanism can effectively reduce computational overhead.
2. To resist the impact of lumped disturbances on trajectory tracking, a framework integrating the SMO with the hybrid event-triggering mechanism is established. The MPC within this framework achieving more precise control while further reducing computational load.

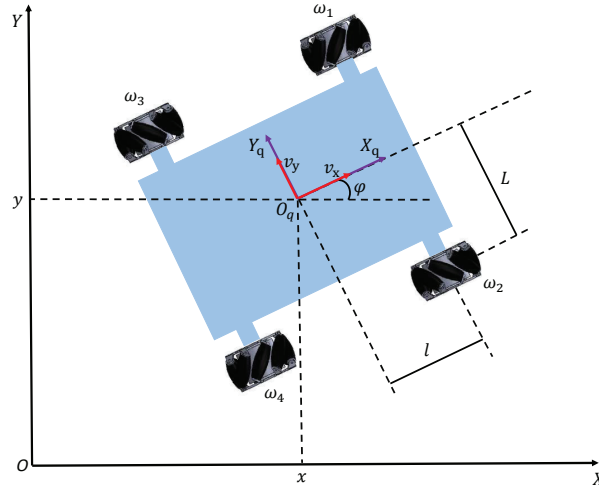


FIGURE 1 The model of the Mecanum-wheeled mobile robot.

3. Compared to existing event-triggered MPC, the effectiveness of the proposed SMO-HETMPC is proved by comparison with the latest high-impact methods^{5,20,28}.

The remaining sections of this paper are planned as follows. Section 2 explains the system description. Section 3 introduces the novel hybrid event-triggered MPC scheme and provides proof that the system avoids Zeno behavior. Section 4 presents the novel SMO and demonstrates its stability by Lyapunov method. Section 5 verifies the effectiveness of the SMO-HETMPC algorithm through experimental experiments and comparisons. Finally, conclusions are presented in Section 6.

2 | MATHEMATICAL MODEL OF MWMP

Fig. 1 shows the motion schematic of the robot, where XOY and $X_qO_qY_q$ respectively represent the inertial coordinate system and robot coordinate system.

2.1 | Kinematics of MWMR

According to the kinematic model of MWMR introduced in¹⁶, the relation between the body velocities of the MWMR, and the angular velocities of the four wheels can be calculated as

$$\begin{bmatrix} v_x \\ v_y \\ v_\varphi \end{bmatrix} = J_r \begin{bmatrix} \omega_1 \\ \omega_2 \\ \omega_3 \\ \omega_4 \end{bmatrix}, \quad (1)$$

where

$$J_r = \frac{r}{4} \begin{bmatrix} 1 & 1 & 1 & 1 \\ -1 & 1 & 1 & -1 \\ \frac{-1}{l+l} & \frac{1}{l+l} & \frac{-1}{l+l} & \frac{1}{l+l} \end{bmatrix} \quad (2)$$

represents the Jacobian matrix, the variable r signifies the radius of the Mecanum wheels, while L and l denote the distances between the wheels and the center of the robot, respectively. The vector $[v_x, v_y, v_\varphi]^T$ represents the robot's velocity components along X_q, Y_q , and the rotational speed around the geometric center of the body, while $[w_1, w_2, w_3, w_4]^T$ represents the angular velocities of four wheels.

Subsequently, the nominal kinematics model of the MWMR is expressed as:

$$\begin{bmatrix} \dot{x} \\ \dot{y} \\ \dot{\varphi} \end{bmatrix} = \begin{bmatrix} \cos(\varphi) & -\sin(\varphi) & 0 \\ \sin(\varphi) & \cos(\varphi) & 0 \\ 0 & 0 & 1 \end{bmatrix} \begin{bmatrix} v_x \\ v_y \\ v_\varphi \end{bmatrix}, \quad (3)$$

where $[x, y, \varphi]^T$ represents the MWMR's pose information in the inertial coordinate system.

2.2 | Dynamics of MWMR

Based on^{34,35}, nominal dynamics model of the MWMR without considering friction can be derived by using Lagrange equation. Hence, the kinetic energy equation of the MWMR is given as follows:

$$K = \frac{1}{2}m(v_x^2 + v_y^2) + \frac{1}{2}J_z v_\varphi^2 + \frac{1}{2}J_\omega(\dot{\theta}_1^2 + \dot{\theta}_2^2 + \dot{\theta}_3^2 + \dot{\theta}_4^2) \quad (4)$$

where the vector $\theta = [\theta_1, \theta_2, \theta_3, \theta_4]^T$ is the angle of four wheels; $\dot{\theta}_i = \omega_i$, $i = 1, 2, 3, 4$; m denotes the total mass of the MWMR; J_z and J_ω denote the moments of the MWMR and wheel inertia around the center of their revolution, respectively.

The energy dissipation due to viscous friction can be expressed as:

$$D = \frac{1}{2}D_\theta(\dot{\theta}_1^2 + \dot{\theta}_2^2 + \dot{\theta}_3^2 + \dot{\theta}_4^2), \quad (5)$$

where D_θ represents the viscous friction coefficient of the wheel. Subsequently, the Lagrange function is formulated as:

$$L = K - V, \quad (6)$$

where V is potential energy and equals to zero. The Euler Lagrangian equation can be constructed as:

$$\frac{\partial}{\partial t} \frac{\partial L}{\partial \dot{\theta}} - \frac{\partial L}{\partial \theta} = \tau - \left(\frac{\partial D}{\partial \dot{\theta}} + F(\dot{\theta}) \right), \quad (7)$$

where the vector $\tau = [\tau_1, \tau_2, \tau_3, \tau_4]^T$ represents the generalized external force exerted by the DC motors, individually corresponding to the four wheels of the MWMR. The static friction be expressed as $F(\dot{\theta}) = [f_{c1} \text{sgn}(\dot{\theta}_1), f_{c2} \text{sgn}(\dot{\theta}_2), f_{c3} \text{sgn}(\dot{\theta}_3), f_{c4} \text{sgn}(\dot{\theta}_4)]$ is generally known, further derivation of Eq. (7) results in:

$$\tau = M\ddot{\theta} + D_\theta\dot{\theta} + F(\dot{\theta}), \quad (8)$$

where

$$M = \begin{bmatrix} A_j + B_j + J_\omega & -B_j & B_j & A_j - B_j \\ -B_j & A_j + B_j + J_\omega & A_j - B_j & B_j \\ B_j & A_j - B_j & A_j + B_j + J_\omega & -B_j \\ A_j - B_j & B_j & -B_j & A_j + B_j + J_\omega \end{bmatrix}, \quad (9)$$

$$A_j = \frac{mr^2}{8}, B_j = \frac{J_z r^2}{16(l+L)^2}.$$

Differentiating (1) and substituting (3) and (8), the nominal dynamics model of the robot can be written as:

$$\begin{bmatrix} \ddot{x} \\ \ddot{y} \\ \ddot{\varphi} \end{bmatrix} = - \left(F^+ (\varphi) \dot{F} (\varphi) + D_\theta F^+ (\varphi) M^{-1} F (\varphi) \right) \begin{bmatrix} \dot{x} \\ \dot{y} \\ \dot{\varphi} \end{bmatrix} + r F^+ (\varphi) M^{-1} (\tau - F(\dot{\theta})), \quad (10)$$

where

$$\begin{aligned}
 F(\varphi) &= \begin{bmatrix} \sqrt{2} \sin(\varphi_a) & -\sqrt{2} \cos(\varphi_a) & -(l+L) \\ \sqrt{2} \cos(\varphi_a) & \sqrt{2} \sin(\varphi_a) & l+L \\ \sqrt{2} \cos(\varphi_a) & \sqrt{2} \sin(\varphi_a) & -(l+L) \\ \sqrt{2} \sin(\varphi_a) & -\sqrt{2} \cos(\varphi_a) & l+L \end{bmatrix}, \\
 F^+(\varphi) &= \\
 &\frac{1}{4} \begin{bmatrix} \sqrt{2} \sin(\varphi_a) & \sqrt{2} \cos(\varphi_a) & \sqrt{2} \cos(\varphi_a) & \sqrt{2} \sin(\varphi_a) \\ -\sqrt{2} \cos(\varphi_a) & \sqrt{2} \sin(\varphi_a) & \sqrt{2} \sin(\varphi_a) & -\sqrt{2} \cos(\varphi_a) \\ \frac{-1}{l+L} & \frac{1}{l+L} & \frac{-1}{l+L} & \frac{1}{l+L} \end{bmatrix}, \\
 \dot{F}(\varphi) &= \dot{\varphi} \begin{bmatrix} \sqrt{2} \cos(\varphi_a) & \sqrt{2} \sin(\varphi_a) & 0 \\ -\sqrt{2} \sin(\varphi_a) & \sqrt{2} \cos(\varphi_a) & 0 \\ -\sqrt{2} \sin(\varphi_a) & \sqrt{2} \cos(\varphi_a) & 0 \\ \sqrt{2} \cos(\varphi_a) & \sqrt{2} \sin(\varphi_a) & 0 \end{bmatrix}, \\
 \varphi_a &= \varphi + \frac{\pi}{4}.
 \end{aligned} \tag{11}$$

By defining the state variable $\mathbf{x} = [x, y, \varphi, \dot{x}, \dot{y}, \dot{\varphi}]^T$ and the control input $\mathbf{u} = \boldsymbol{\tau} - F(\boldsymbol{\theta})$, the state equation of the MWMR system can be simplified to the following form:

$$\dot{\mathbf{x}} = \mathbf{A}\mathbf{x} + \mathbf{B}\mathbf{u}, \tag{12}$$

where

$$\begin{aligned}
 \mathbf{A} &= \begin{bmatrix} 0 & \mathbf{E} \\ 0 & -(F^+(\varphi)\dot{F}(\varphi) + D_\theta F^+(\varphi)M^{-1}F(\varphi)) \end{bmatrix} \in \mathbb{R}^{6 \times 6}, \\
 \mathbf{B} &= \begin{bmatrix} 0 \\ rF^+(\varphi)M^{-1} \end{bmatrix} \in \mathbb{R}^{6 \times 4},
 \end{aligned} \tag{13}$$

and $\mathbf{E} \in \mathbb{R}^{3 \times 3}$ is an identity matrix.

Remark 1: Define the notation \mathbf{x} and \mathbf{r} as the system state and the reference state respectively. Then, the tracking error of the system can be represented as:

$$\mathbf{e} = \mathbf{x} - \mathbf{r}. \tag{14}$$

At this point, the tracking problem in MWMR can be reformulated as the stability problem of (14).

3 | HYBRID EVENT-TRIGGERED MPC

3.1 | The QP formulation for model predictive controller

It is widely acknowledged MPC falls under the category of optimal control techniques. In this paper, a time series $\{t_k\}$, $k \in \mathbb{N}$ is defined to record the triggered moments at which the optimal control problem needs to be addressed. Then, the discrete expression of the system (12) at one moment could be described as:

$$\mathbf{x}(t_k + 1) = \mathbf{G}_k \mathbf{x}(t_k) + \mathbf{H}_k \mathbf{u}(t_k), \tag{15}$$

where

$$\mathbf{G}_k = (\mathbf{E} + \mathbf{T}\mathbf{A}), \quad \mathbf{H}_k = \mathbf{T}\mathbf{B}, \tag{16}$$

and the notation \mathbf{T} is the sampling time. Define N_p as the prediction horizon of the system. Then, the following cost function can be formulated:

$$\begin{aligned}
 J(\mathbf{x}(s|t_k), \Delta \mathbf{u}(s|t_k)) &= \\
 &\sum_{j=1}^{N_p} \|\mathbf{x}(t_k + j|t_k) - \mathbf{r}(t_k + j)\|_Q^2 + \sum_{j=0}^{N_p-1} \|\Delta \mathbf{u}(t_k + j|t_k)\|_R^2,
 \end{aligned} \tag{17}$$

where Q and R denote positive definite matrix of corresponding dimension. The input increment vector $\Delta \mathbf{u}(t_k + j|t_k) = \mathbf{u}(t_k + j|t_k) - \mathbf{u}(t_k + j - 1|t_k)$, where $\mathbf{u}(t_k + j|t_k)$ is the predicted control input vector.

Thus, the optimization problem can be established as follows:

$$\begin{aligned}
\Delta \mathbf{u}^*(s|t_k) &= \min_{\Delta \mathbf{u}(s|t_k)} J(\mathbf{x}(s|t_k), \Delta \mathbf{u}(s|t_k)), \\
\text{s.t.} \\
s &\in [t_k, t_k + N_p], \\
\mathbf{x}_{\min} &\leq \mathbf{x}(s|t_k) \leq \mathbf{x}_{\max}, \\
\mathbf{u}_{\min} &\leq \mathbf{u}(s|t_k) \leq \mathbf{u}_{\max}, \\
\Delta \mathbf{u}_{\min} &\leq \Delta \mathbf{u}(s|t_k) \leq \Delta \mathbf{u}_{\max},
\end{aligned} \tag{18}$$

where \mathbf{x}_{\min} , \mathbf{x}_{\max} , \mathbf{u}_{\min} , \mathbf{u}_{\max} , $\Delta \mathbf{u}_{\min}$ and $\Delta \mathbf{u}_{\max}$ are the corresponding lower and upper bounds of variables. The $\Delta \mathbf{u}^*(s|t_k)$ obtained by solving the optimal control problem (18) will be used as the control input increment to the system (15).

3.2 | Hybrid event-triggered mechanism

A controller capable of solving the trajectory tracking problem can be derived based on Section 3.1. However, solving the optimization problem (18) frequently can be computationally burdensome, hence the hybrid event-triggered mechanism is introduced in this paper. Initially, after solving the optimal control problem at the moment t_k , the error between the actual system state and the reference state is defined as:

$$e(s|t_k) = \mathbf{x}(s|t_k) - \mathbf{r}(s), \quad s \in [t_k, t_k + N_p]. \tag{19}$$

Then, two events are defined as:

$$C = \{s > t_k \mid \|e(s|t_k)\|_p > \varepsilon\}, \tag{20a}$$

$$F = \{\mu > t_k + T \mid \|e(\mu|t_k) - e(\mu - T|t_k)\|_p > \sigma\}, \tag{20b}$$

in which the event C maintains the system's adherence to the reference state \mathbf{r} , whereas the event F ensures the continuous approach towards the reference state. Then, the instants for triggering are defined as:

$$\bar{t}_{k+1} \triangleq \min(C \cap F). \tag{21}$$

Remark 2: Compared to traditional event-triggering condition C , the proposed hybrid event-triggered mechanism introduces the novel condition F which is determined by evaluating the gradients of the differences between the actual state and the reference state at two consecutive sample instances.

The solving of the optimization problem also occurs in the case of fixed moments with a period in the prediction time domain N_p . Thus, the next triggered instant for the time series $\{t_k\}$ is finally expressed as:

$$t_{k+1} = \min\{\bar{t}_{k+1}, t_k + N_p\}. \tag{22}$$

Remark 3: Zeno behavior commonly occurs in event-triggered mechanisms, representing 0 trigger or infinite trigger within a confined time frame in event-triggered control. In the experiments of this paper, a fixed sampling time T is set, i.e., the system regularly collects the current state and judges whether the triggering condition is satisfied. The interval between two events is represented by $\inf\{t_{k+1} - t_k\} = T$ for the minimum time and $\sup\{t_{k+1} - t_k\} = N_p, k \in N$ for the maximum time, respectively. Therefore, the proposed event-triggered mechanism is Zeno-free.

4 | SLIDING MODE OBSERVER

In order to attain the intended control effect, it is necessary to account for unknown disturbances and model uncertainties, referred to as aggregate disturbances. Within this section, a SMO algorithm is developed to estimate the combined perturbations within the MWMR kinematic model (3). This perturbation estimation is applied to mitigate the perturbation's impact on the system, thus enhancing the system's robustness. Considering external interferences and model uncertainties, the kinematic model of MWMR should be derived under the following assumption:

Assumption 1: The unknown disturbances and model uncertainties in the system are all bounded.

Considering the aggregate disturbances, the relation (1) can be rewritten as:

$$\begin{bmatrix} v_x \\ v_y \\ \omega \end{bmatrix} = J_r \begin{bmatrix} w_1 \\ w_2 \\ w_3 \\ w_4 \end{bmatrix} + \begin{bmatrix} f_x \\ f_y \\ f_\omega \end{bmatrix}, \quad (23)$$

where $[f_x, f_y, f_\omega]^T$ denotes the aggregate disturbances in different velocity directions of the robot centroid. Then, the kinematic model can be written as:

$$\begin{bmatrix} \dot{x} \\ \dot{y} \\ \dot{\varphi} \end{bmatrix} = \begin{bmatrix} \cos(\varphi) & -\sin(\varphi) & 0 \\ \sin(\varphi) & \cos(\varphi) & 0 \\ 0 & 0 & 1 \end{bmatrix} \left(J_r \begin{bmatrix} w_1 \\ w_2 \\ w_3 \\ w_4 \end{bmatrix} + \begin{bmatrix} f_x \\ f_y \\ f_\omega \end{bmatrix} \right). \quad (24)$$

Then, the kinematic model (24) can be reformulated in the subsequent manner:

$$\dot{\mathbf{z}} = \bar{\mathbf{B}}\mathbf{v} + \mathbf{D}\mathbf{f}, \quad (25)$$

where

$$\bar{\mathbf{B}} = \frac{r}{4} \begin{bmatrix} \cos(\varphi) & -\sin(\varphi) & 0 \\ \sin(\varphi) & \cos(\varphi) & 0 \\ 0 & 0 & 1 \end{bmatrix} \begin{bmatrix} 1 & 1 & 1 & 1 \\ -1 & 1 & 1 & -1 \\ \frac{-1}{l+L} & \frac{1}{l+L} & \frac{-1}{l+L} & \frac{1}{l+L} \end{bmatrix}, \quad (26)$$

$$\mathbf{D} = \begin{bmatrix} \cos(\varphi) & -\sin(\varphi) & 0 \\ \sin(\varphi) & \cos(\varphi) & 0 \\ 0 & 0 & 1 \end{bmatrix},$$

$\mathbf{v} = [w_1, w_2, w_3, w_4]^T$ and $\mathbf{z} = [x, y, \varphi]^T$. Then, the sliding surface can be designed as:

$$\mathbf{s} = \mathbf{z} - \hat{\mathbf{z}}, \quad (27)$$

where $\mathbf{s} = [s_1, s_2, s_3]^T$, and $\hat{\mathbf{z}} = [\hat{x}, \hat{y}, \hat{\varphi}]^T$ denote the estimate value of the position and direction angle. Then, the estimated state equation is considered as:

$$\dot{\hat{\mathbf{z}}} = \bar{\mathbf{B}}\mathbf{v} + K_1(e^{K_2 s} - 1) + K_3 \mathbf{sgn}(\mathbf{s}), \quad (28)$$

in which $K_i = \text{diag}(k_{i1}, k_{i2}, k_{i3})$, $i = 1, 2, 3$ is appropriate positive definite matrix, $\mathbf{sgn}(\mathbf{s}) \triangleq [\text{sgn}(s_1), \text{sgn}(s_2), \text{sgn}(s_3)]^T$ is the symbolic function.

By subtracting (28) from (25), the observation error can be obtained as:

$$\dot{\mathbf{s}} = \mathbf{D}\mathbf{f} - K_1(e^{K_2 s} - 1) - K_3 \mathbf{sgn}(\mathbf{s}). \quad (29)$$

Once the system reaches the sliding surface, then

$$\mathbf{s} = \dot{\mathbf{s}} = 0. \quad (30)$$

Combining (29) and (30), yields

$$\hat{\mathbf{f}} = \mathbf{D}^{-1}[K_1(e^{K_2 s} - 1) + K_3 \mathbf{sgn}(\mathbf{s})]. \quad (31)$$

Theorem 1: If (27) spontaneously approaches zero, it means that the proposed SMO (28) enables accurate estimation of the unknown external disturbances and uncertainties affecting the MWMR system (25).

Proof. Consider a Lyapunov function:

$$V = \frac{1}{2} \mathbf{s}^T \mathbf{s}. \quad (32)$$

Obviously, the function V is positive definite. Define $\mathbf{d}_{\text{dis}} = D\mathbf{f} = [d_{1\text{dis}}, d_{2\text{dis}}, d_{3\text{dis}}]$. Differentiating Eq. (32) with respect to time yields:

$$\begin{aligned}
\dot{V} &= \frac{1}{2} \dot{\mathbf{s}}^T \mathbf{s} + \frac{1}{2} \mathbf{s}^T \dot{\mathbf{s}} \\
&= \mathbf{s}^T \dot{\mathbf{s}} \\
&= \mathbf{s}^T [D\mathbf{f} - K_1(e^{K_2 s} - 1) - K_3 \text{sgn}(\mathbf{s})] \\
&= \mathbf{s}^T D\mathbf{f} - \mathbf{s}^T K_1(e^{K_2 s} - 1) - \mathbf{s}^T K_3 \text{sgn}(\mathbf{s}) \\
&= \sum_{i=1}^3 s_i d_{i\text{dis}} - \sum_{i=1}^3 k_{1i}(e^{k_{2i}s_i} - 1) - \sum_{i=1}^3 s_i k_{3i} \text{sgn}(s_i) \\
&\leq \sum_{i=1}^3 s_i d_{i\text{dis}} - \sum_{i=1}^3 s_i k_{3i} \text{sgn}(s_i) \\
&\leq \sum_{i=1}^3 |s_i| |d_{i\text{dis}}| - \sum_{i=1}^3 |s_i| k_{3i}
\end{aligned} \tag{33}$$

According to Assumptions 1, it can be deduced that \mathbf{d}_{dis} is bounded, so the nominal values of definite matrix K_3 can be designed to make $|d_{i\text{dis}}| < \bar{k}_3 i$, $i = 1, 2, 3$. In this case, demonstrating $\dot{V} < 0$ is readily achieved, indicating the convergence of all sliding mode variables s_i , $i = 1, 2, 3$ towards the internal confines of the boundary layer. As the thickness of the boundary layer approaches zero, the sliding mode variables s_i also converge towards zero. Consequently, affirming the system's stability.

This ends the proof. \square

In summary, the MPC (18), event-triggered mechanism (20) and SMO (28) form the basis of the sliding mode observer-based event-triggered model predictive control algorithm, which is formally illustrated in Algorithm 1.

Algorithm 1 SMO-HETMPC algorithm

- 1: Initialization.
 - 2: **while** maximum value of set time not reached **do**
 - 3: Solve the optimization problem at t_k to obtain $\Delta \mathbf{u}^*(t_k)$.
 - 4: Apply the disturbance-compensated control input $\mathbf{u}^*(t_k|t_k)$.
 - 5: Estimate the next moment of disturbance $\hat{\mathbf{f}}$.
 - 6: $s = t_k + 1$.
 - 7: **while** the event (20) is not triggered **do**
 - 8: **if** $s < t_k + N_p$ **then**
 - 9: Apply the disturbance-compensated control input $\mathbf{u}^*(s|t_k)$.
 - 10: Estimate the next moment of disturbance $\hat{\mathbf{f}}$.
 - 11: $s = s + 1$.
 - 12: **else**
 - 13: Break.
 - 14: **end if**
 - 15: **end while**
 - 16: $t_k = s$.
 - 17: **end while**
-

5 | EXPERIMENT RESULTS

In this section, in order to demonstrate the advantages of the proposed SMO-HETMPC algorithm, two types of experiments were conducted. Firstly, comparative simulation experiments are conducted based on Matlab. In which, the results of MPC⁵,

ETMPC²⁰, HETMPC, and ESO-ETMPC²⁸ are compared in the case with external disturbance. Secondly, to demonstrate the effectiveness of the algorithm, a robot experiment based on CoppeliaSim is also set up in this section.

5.1 | Comparative simulation experiments

In the simulation case, a lemniscate-shape trajectory is set as:

$$\mathbf{r}_1(t) = \begin{bmatrix} x_r(t) \\ y_r(t) \\ \varphi_r(t) \end{bmatrix} = \begin{bmatrix} 3\cos(0.1t) \text{ m} \\ \sin(0.2t) \text{ m} \\ \frac{\pi}{2}\sin(0.1t) \text{ rad} \end{bmatrix}. \quad (34)$$

The parameters are set to: $r = 0.05\text{m}$, $L = 0.35\text{m}$, $l = 0.25\text{m}$. The total control time T_c of the system is 160s and the sampling time T is 0.1s. The parameters of the model predictive controller are chosen as: $N_p = 5$, $\mathbf{Q} = \text{diag}(300, 300, 300, 50, 50, 50)$, $\mathbf{P} = \text{diag}(1, 1, 1, 1, 1, 1)$. The parameters of SMO (28) are set to: $K_1 = K_2 = \text{diag}(5, 5, 5)$ and $K_3 = 0.001\text{diag}(1, 1, 1)$. The lumped disturbances are set as

$$\mathbf{f}(t) = \begin{bmatrix} 0.2\cos(0.01t) + 0.035\sin(0.05t) \\ 0.2\sin(0.02t) \\ 0.05\sin(0.01t) \end{bmatrix}. \quad (35)$$

The initial position and orientation angle of the tracking robot is set to $(x, y, \varphi) = (2.5 \text{ m}, 0 \text{ m}, 0 \text{ rad})$. Fig. 2 shows the visualization tracking outcomes for the lemniscate-shaped trajectory. While Fig. 3 and Fig. 4 illustrate the system's error fluctuations and the integral absolute tracking errors (IAE) when employing aforementioned controllers. It is easy to find that those controllers equipped with the observer can better resist the disturbance and track the trajectory. Obviously, the SMO-HETMPC demonstrates the capacity to reduce the error to nearly zero, thereby affirming its effectiveness. Moreover, Fig. 5 illustrates the estimations of the lumped disturbances. Although the lumped disturbances change irregularly, the designed SMO retains the capability to swiftly and precisely estimate the disturbance value, demonstrating minimal estimation errors or chattering. The triggered times (TT) comparison of the four mentioned MPC strategies are recorded in Fig. 6 and Table 1. It can be observed from Fig. 6 and Table 1 that, compared with the ETMPC and HETMPC, the observer-based MPC strategy effectively estimates the overall lumped disturbances, significantly reducing the frequency of event triggers. However, compared to EMO-ETMPC, the proposed algorithm demonstrates fewer triggering instances while achieving similar tracking performance, showcasing its advantages.

TABLE 1 Comparison of triggering times.

Method	Triggered times	Improvement ¹
MPC	1595	-
ETMPC	1555	2.51%
HETMPC	958	39.9%
ESO-ETMPC	1210	24.1%(22.2%) ²
SMO-HETMPC	585	63.3%(38.9%) ²

¹ The improvement relative to MPC.

² The improvement of this algorithm relative to the algorithm without observer.

For further assessment of the algorithm's stability and reliability, an additional set of 30 independent repeated experiments is conducted. The experiments are conducted with different initial setpoints for each trial. In the case where the parameters of the robot and controller remain unchanged, the initial position for the i th experiment is set to $(x, y, \varphi) = (2.5 + 0.01i \text{ m}, 0 \text{ m}, 0 \text{ rad})$, with the lumped disturbances configured as

$$\mathbf{f}(t) = \frac{i}{10} \begin{bmatrix} 0.2\cos(0.01t) + 0.035\sin(0.05t) \\ 0.2\sin(0.02t) \\ 0.05\sin(0.01t) \end{bmatrix}. \quad (36)$$

Table 2 provides a comprehensive summary, outlining statistical metrics and relevant numerical. Besides the mentioned TT and IAE, we also introduce the integrated square error (ISE) in Table 2, providing the mean values of these three metrics along

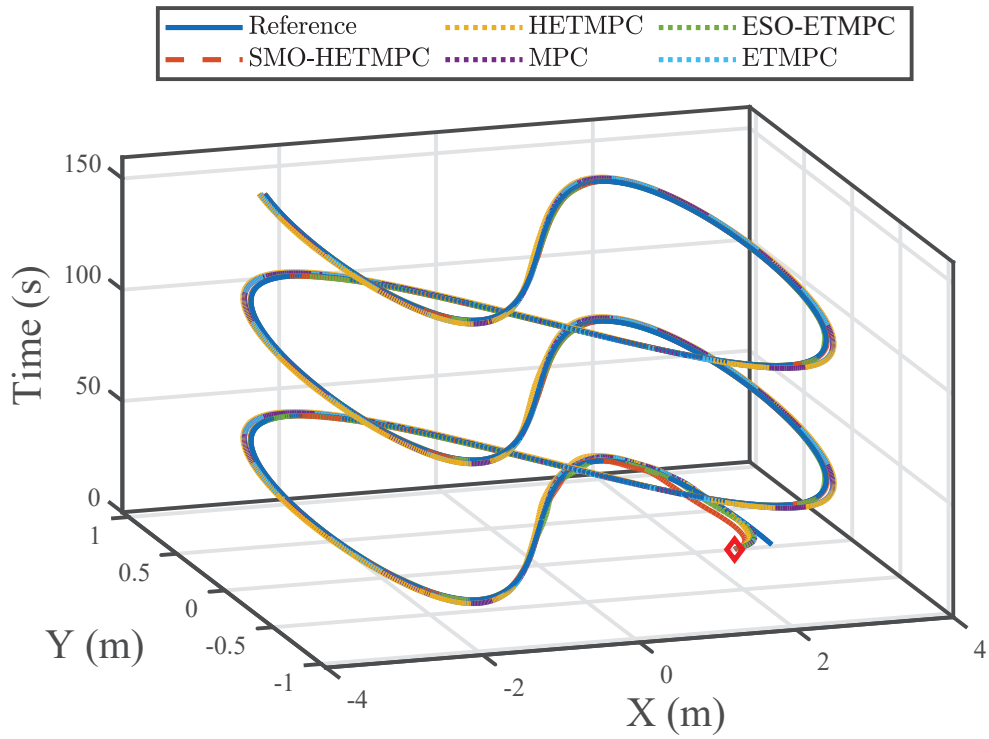


FIGURE 2 Trajectory tracking result comparisons of lemniscate reference trajectory.

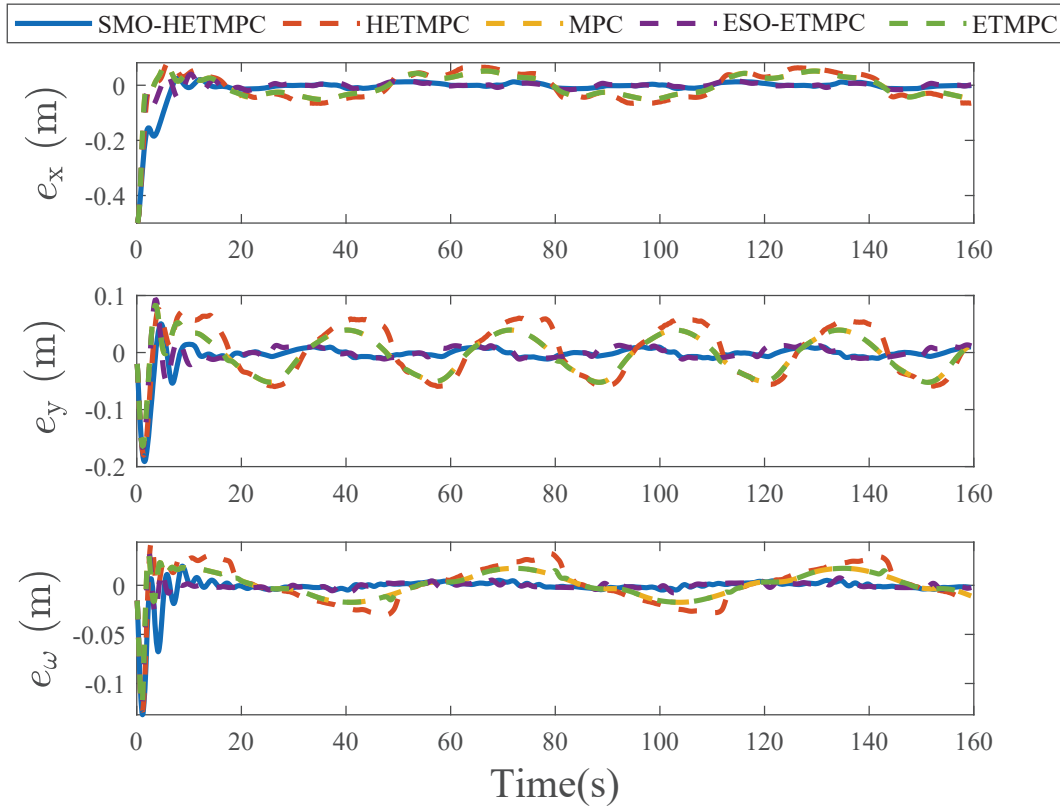


FIGURE 3 Curve graph depicting the errors variation over time.

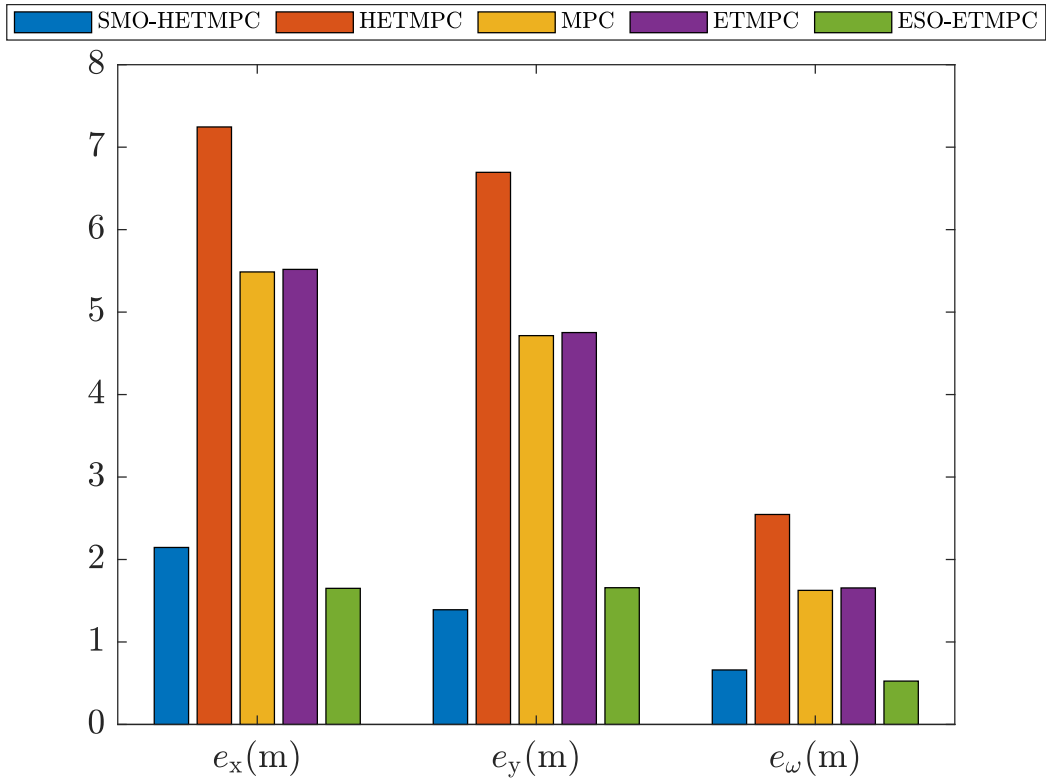


FIGURE 4 The integral absolute tracking errors.

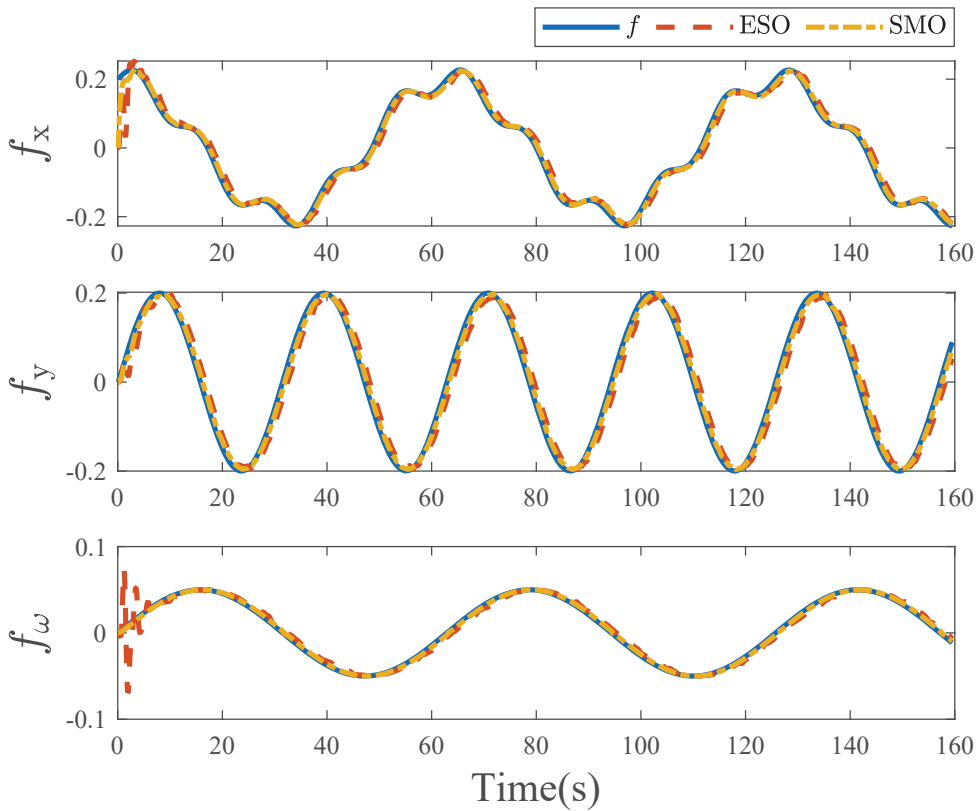


FIGURE 5 Estimations of lumped disturbances.

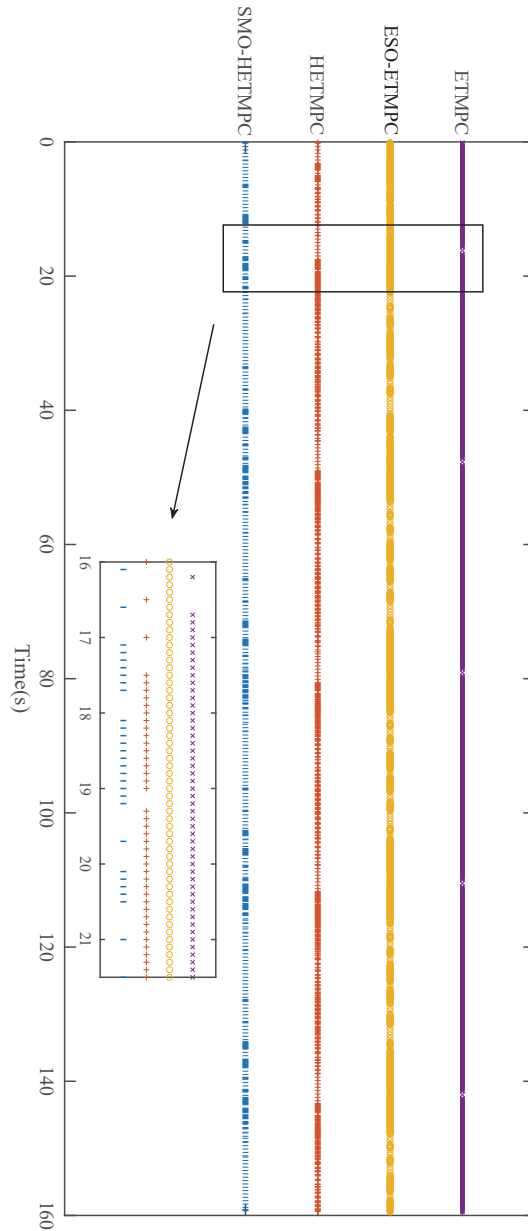


FIGURE 6 Triggering instants and triggering intervals.

with their 95% confidence intervals. Fig. 7 offers a comparative visualization of IAE and ISE. From Table 2, it can be noted that the observer-based controllers exhibit better stability when facing various disturbances, while SMO-HETMPC additionally shows lower trigger frequency, suggesting reduced computational resource consumption. Furthermore, the proposed algorithm exhibits consistent performance across 30 independent repeated comparative experiments, further demonstrating its stability and robustness.

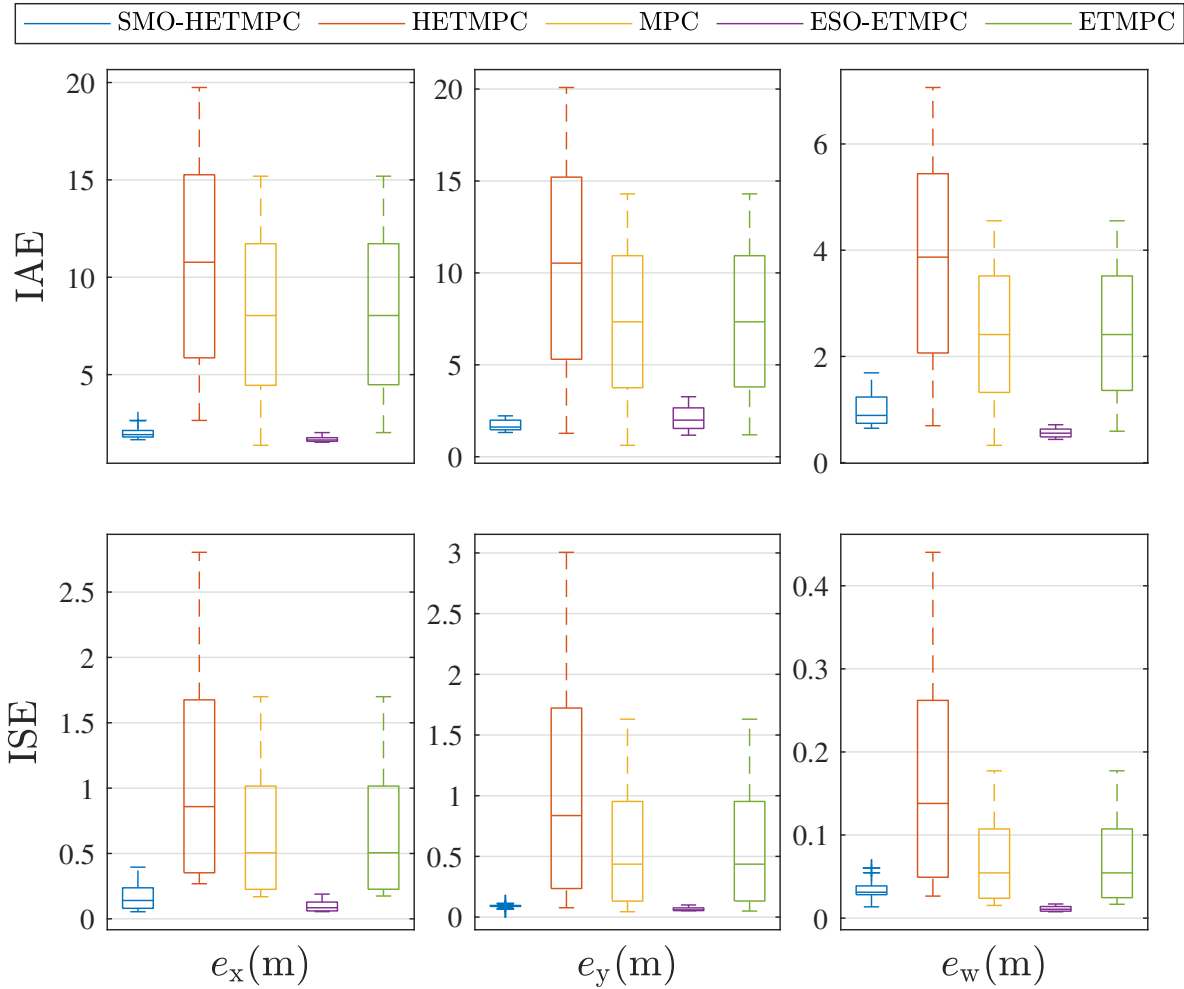


FIGURE 7 Comparisons of multidimensional IAE and ISE in repeated experiments for tracking lemniscate reference trajectory.

5.2 | Robot experiment

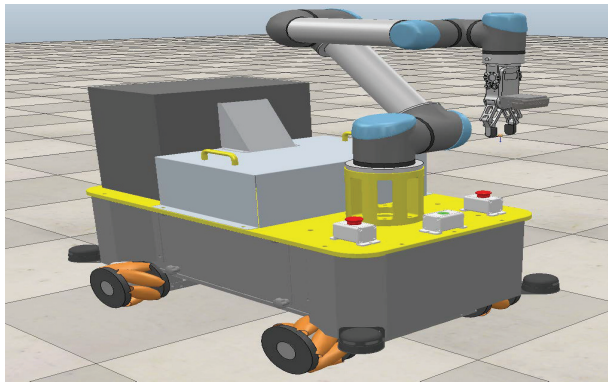
To further validate the feasibility of the proposed algorithm, this section observes the tracking performance of the SMO-HETMPC when applied to the robotic platform. The robot utilized in this experiment is a MWMR model autonomously developed based on the CoppeliaSim platform. The advantage of this platform is its ability to provide a realistic experimental environment while obtaining accurate position and velocity information of the robot. Meanwhile, in order to validate the robustness of the proposed algorithm, a different trajectory is employed in this experiment as:

$$\mathbf{r}_2(t) = \begin{bmatrix} x_r(t) \\ y_r(t) \\ \varphi_r(t) \end{bmatrix} = \begin{bmatrix} 3\cos(0.1t) - 2 \text{ m} \\ 3\sin(0.1t) \text{ m} \\ \frac{\pi}{2}\sin(0.1t) \text{ rad} \end{bmatrix} \quad (37)$$

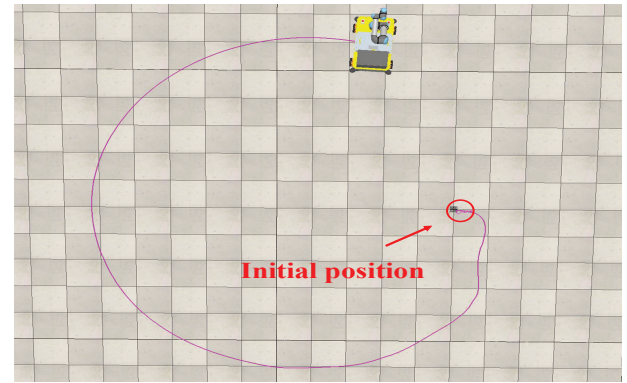
The scenario setup for the robot experiment is shown in Fig. 8. Fig. 9 and Fig. 10 illustrate the tracking result and the temporal evolution of error, respectively. It is evident that the robot rapidly converges in minimizing its positional error, consistently maintaining alignment with the desired trajectory. Moreover, the proposed algorithm effectively reduces the expected MPC triggers occurrences from 800 to 309, demonstrating its effectiveness and robustness.

TABLE 2 Comparisons of tracking performance of the MWMR in independent repeated experiments.

Method	TT		Direction	IAE		ISE	
	M-TT	CI		M-IAE	CI	M-ISE	CI
MPC	1595.0	[1595.0, 1595.0]	X-axis	8.109	[6.527, 9.691]	0.659	[0.479, 0.840]
			Y-axis	7.359	[5.793, 8.925]	0.578	[0.392, 0.765]
ETMPC	1507.5	[1429.8, 1585.2]	X-axis	8.168	[6.618, 9.719]	0.661	[0.480, 0.841]
			Y-axis	7.418	[5.884, 8.953]	0.579	[0.393, 0.765]
HETMPC	943.27	[913.07, 973.47]	X-axis	10.75	[8.766, 12.74]	1.089	[0.791, 1.388]
			Y-axis	10.38	[8.235, 12.53]	1.060	[0.722, 1.398]
ESO-ETMPC	1239.9	[1153.2, 1326.6]	X-axis	1.687	[1.635, 1.738]	0.098	[0.082, 0.114]
			Y-axis	2.093	[1.847, 2.338]	0.066	[0.060, 0.071]
SMO-HETMPC	692.63	[663.21, 722.06]	X-axis	2.001	[1.895, 2.108]	0.169	[0.131, 0.207]
			Y-axis	1.752	[1.634, 1.869]	0.090	[0.086, 0.095]



(a)



(b)

FIGURE 8 Motion control scenario. (a) MWMR model. (b) Robot trajectory record.

6 | CONCLUSION

This study presents a novel trajectory tracking approach for MWMR by amalgamating SMO with hybrid event-triggered MPC. To address the frequent triggering issue in conventional ETMPC affected by lumped disturbances, a hybrid event triggering mechanism is proposed, which determines whether to trigger or not through two types of events together. Additionally, the SMO is introduced to estimate and counteract the impact of lumped disturbances. This approach reduces communication load, energy consumption, and computational burden by minimizing the number of times optimization problems need solving. Theoretical analysis demonstrates the viability of the new method and the stability of the perturbed system. Finally, a series of experiments confirm the effectiveness and superiority of the proposed algorithm.

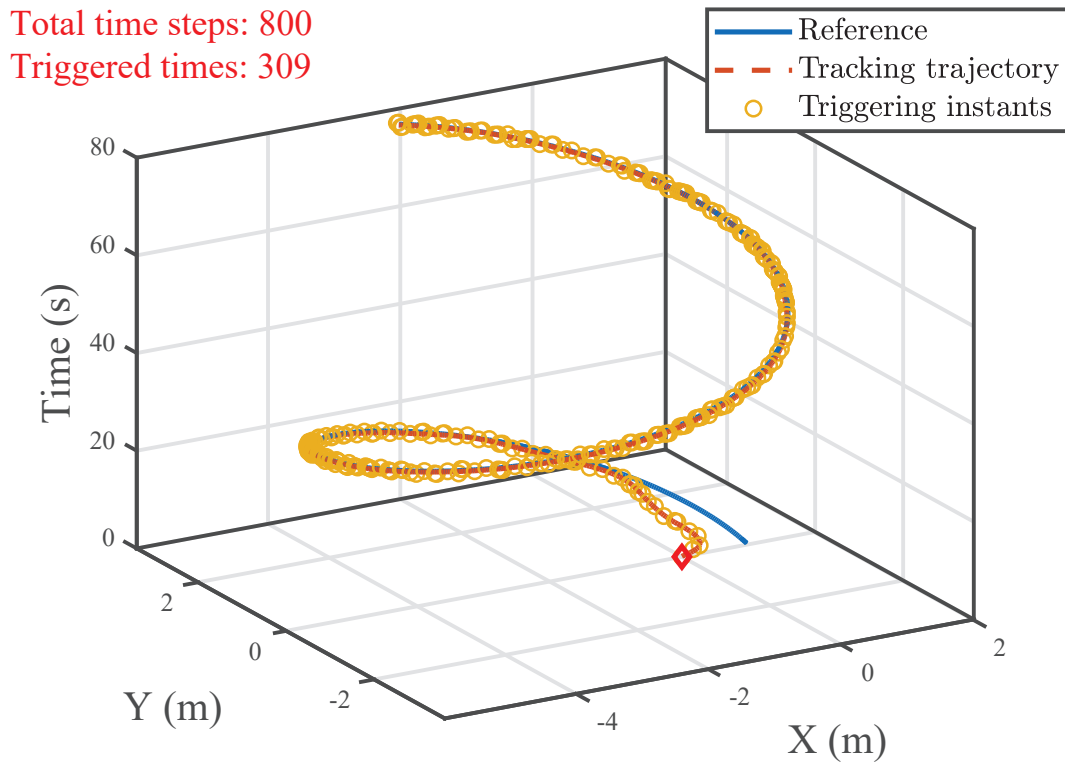


FIGURE 9 Temporal evolution of robot trajectory in 3D space.

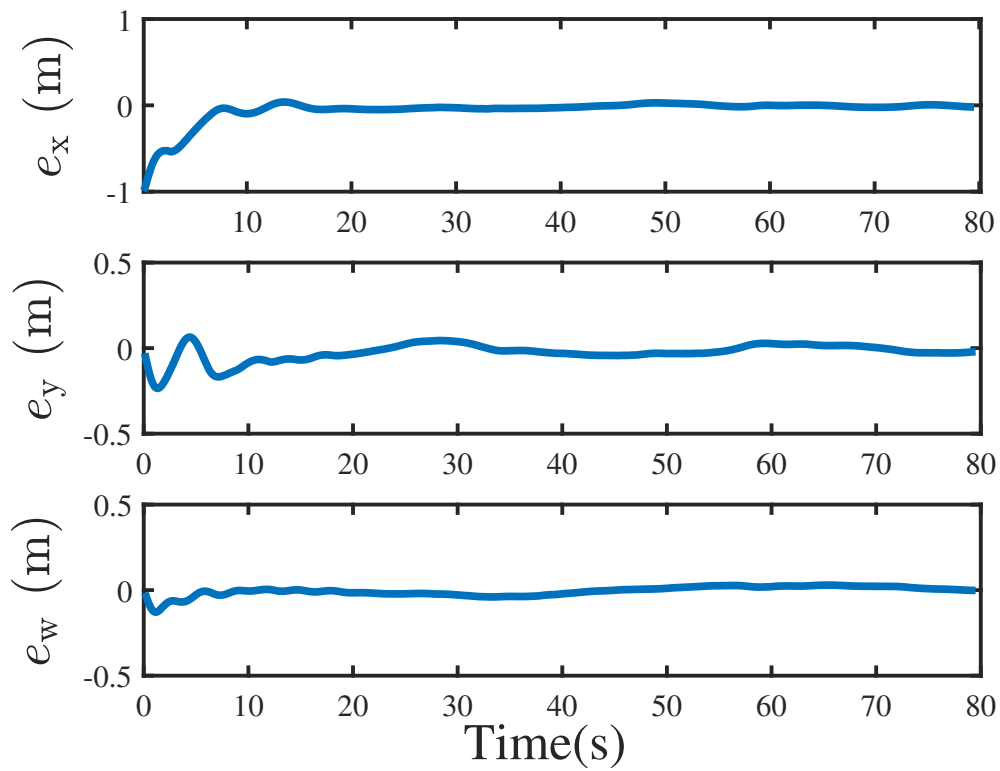


FIGURE 10 Robot pose tracking errors on circular trajectory.

ACKNOWLEDGMENTS

This research is funded by the Science and Technology Planning Project of Guangdong Province, China (grant numbers 2022A1515110566, 2023A1515011574, 2019A050520001), the STU Scientific Research Initiation Grant NTF21052.

CONFLICT OF INTEREST STATEMENT

The authors declare no potential conflict of interests.

References

1. Li Y, Ge S, Dai S, et al. Kinematic modeling of a combined system of multiple mecamum-wheeled robots with velocity compensation. *Sensors*. 2019;20(1):75. doi: 10.3390/s20010075
2. Mellah S, Graton G, El Adel EM, Ouladsine M, Planchais A. Health state monitoring of 4-Mecanum wheeled mobile robot actuators and its impact on the robot behavior analysis. *J. Intell. Robot. Syst.*. 2021;102(4):86. doi: 10.1007/s10846-021-01446-7
3. Serrano ME, Gandolfo DC, Scaglia GJ. Trajectory tracking controller for unmanned helicopter under environmental disturbances. *ISA Trans.*. 2020;106:171–180. doi: 10.1016/j.isatra.2020.06.026
4. Jing C, Xu H, Niu X. Adaptive sliding mode disturbance rejection control with prescribed performance for robotic manipulators. *ISA Trans.*. 2019;91:41–51. doi: 10.1016/j.isatra.2019.01.017
5. Wang D, Wei W, Yeboah Y, Li Y, Gao Y. A robust model predictive control strategy for trajectory tracking of omnidirectional mobile robots. *Journal of Intelligent & Robotic Systems*. 2020;98:439–453. doi: 10.1007/s10846-019-01083-1
6. Wu C, Tang X, Xu X. Model Predictive Controller Design Based on Residual Model Trained by Gaussian Process for Robots. *Journal of Marine Science and Engineering*. 2023;11(5):893. doi: 10.3390/jmse11050893
7. Yuan Z, Tian Y, Yin Y, Wang S, Liu J, Wu L. Trajectory tracking control of a four Mecanum wheeled mobile platform: an extended state observer-based sliding mode approach. *IET Contr. Theory Appl.*. 2020;14(3):415–426. doi: 10.1049/iet-cta.2018.6127
8. Köhler J, Müller MA, Allgöwer F. Nonlinear reference tracking: An economic model predictive control perspective. *IEEE Transactions on Automatic Control*. 2019;64(1):254–269. doi: 10.1109/TAC.2018.2800789
9. Gao Y, Wei W, Wang X, Wang D, Li Y, Yu Q. Trajectory tracking of multi-legged robot based on model predictive and sliding mode control. *Information Sciences*. 2022;606:489–511. doi: 10.1016/j.ins.2022.05.069
10. Hu C, Zhao L, Qu G. Event-triggered model predictive adaptive dynamic programming for road intersection path planning of unmanned ground vehicle. *IEEE Transactions on Vehicular Technology*. 2021;70(11):11228–11243. doi: 10.1109/TVT.2021.3111692
11. Stomberg G, Ebel H, Faulwasser T, Eberhard P. Cooperative distributed MPC via decentralized real-time optimization: Implementation results for robot formations. *Control Engineering Practice*. 2023;138:105579. doi: 10.1016/j.conengprac.2023.105579
12. Huang C, Shi Q, Ding W, Mei P, Karimi HR. A robust MPC approach for platooning control of automated vehicles with constraints on acceleration. *Control Engineering Practice*. 2023;139:105648. doi: 10.1016/j.conengprac.2023.105648
13. Vargas S, Becerra HM, Hayet JB. MPC-based distributed formation control of multiple quadcopters with obstacle avoidance and connectivity maintenance. *Control Engineering Practice*. 2022;121:105054. doi: 10.1016/j.conengprac.2021.105054

14. Martinsen AB, Lekkas AM, Gros S. Reinforcement learning-based NMPC for tracking control of ASVs: Theory and experiments. *Control Engineering Practice*. 2022;120:105024. doi: 10.1016/j.conengprac.2021.105024
15. Chai R, Tsourdos A, Gao H, Xia Y, Chai S. Dual-Loop Tube-Based Robust Model Predictive Attitude Tracking Control for Spacecraft With System Constraints and Additive Disturbances. *IEEE Transactions on Industrial Electronics*. 2022;69(4):4022-4033. doi: 10.1109/TIE.2021.3076729
16. Wang D, Wei W, Wang X, et al. Formation control of multiple mecanum-wheeled mobile robots with physical constraints and uncertainties. *Applied Intelligence*. 2021;52(3):2510-2529. doi: 10.1007/s10489-021-02459-3
17. Hariprasad K, Bhartiya S. An Efficient and Stabilizing Model Predictive Control of Switched Systems. *IEEE Transactions on Automatic Control*. 2017;62(7):3401-3407. doi: 10.1109/TAC.2016.2613909
18. Fukushima H, Kon K, Matsuno F. Model Predictive Formation Control Using Branch-and-Bound Compatible With Collision Avoidance Problems. *IEEE Transactions on Robotics*. 2013;29(5):1308-1317. doi: 10.1109/TRO.2013.2262751
19. Liu D, Shen M, Jing Y, Wang QG. Distributed Optimization of Nonlinear Multiagent Systems via Event-Triggered Communication. *IEEE Transactions on Circuits and Systems II: Express Briefs*. 2023;70(6):2092-2096. doi: 10.1109/TC-SII.2022.3225800
20. Chen J, Tian E, Luo Y. Event-triggered model predictive control for series-series resonant ICPT systems in electric vehicles: A data-driven modeling method. *Control Engineering Practice*. 2024;142:105752. doi: 10.1016/j.conengprac.2023.105752
21. Wan X, Wei F, Zhang CK, Wu M. Networked Output-Feedback MPC: A Bounded Dynamic Variable and Time-Varying Threshold-Dependent Event-Based Approach. *IEEE Transactions on Cybernetics*. 2022:1-12. doi: 10.1109/TCYB.2022.3220515
22. Zhou Z, Rother C, Chen J. Event-Triggered Model Predictive Control for Autonomous Vehicle Path Tracking: Validation Using CARLA Simulator. *IEEE Transactions on Intelligent Vehicles*. 2023;8(6):3547-3555. doi: 10.1109/TIV.2023.3266941
23. Xu Z, He N, He L, Ma K. Event-Based MPC for Nonlinear Systems with Additive Disturbances: A Quasi-Differential Type Approach. *ISA Transactions*. 2022;128:136-143. doi: 10.1016/j.isatra.2021.11.009
24. Gurumurthy G, Das DK. Terminal sliding mode disturbance observer based adaptive super twisting sliding mode controller design for a class of nonlinear systems. *European Journal of Control*. 2021;57:232-241. doi: 10.1016/j.ejcon.2020.05.004
25. Yuan Z, Tian Y, Yin Y, Wang S, Liu J, Wu L. Trajectory tracking control of a four mecanum wheeled mobile platform: an extended state observer-based sliding mode approach. *IET Control Theory & Applications*. 2020;14(3):415-426. doi: 10.1049/iet-cta.2018.6127
26. Li P, Wang T, Kang Y, Li K, Zhao YB. Event-based model predictive control for nonlinear systems with dynamic disturbance. *Automatica*. 2022;145:110533. doi: 10.1016/j.automatica.2022.110533
27. Yoo J, Johansson KH. Event-Triggered Model Predictive Control With a Statistical Learning. *IEEE Transactions on Systems, Man, and Cybernetics: Systems*. 2021;51(4):2571-2581. doi: 10.1109/TSMC.2019.2916626
28. Liu X, Qiu L, Wu W, et al. Event-Triggered ESO-Based Robust MPC for Power Converters. *IEEE Transactions on Industrial Electronics*. 2023;70(2):2144-2152. doi: 10.1109/TIE.2022.3167135
29. Li P, Kang Y, Wang T, Zhao YB. Disturbance Prediction-Based Adaptive Event-Triggered Model Predictive Control for Perturbed Nonlinear Systems. *IEEE Transactions on Automatic Control*. 2023;68(4):2422-2429. doi: 10.1109/TAC.2022.3169905
30. Liu Y, Liu J, Wang QG, Yu J. Adaptive Command Filtered Backstepping Tracking Control for AUVs Considering Model Uncertainties and Input Saturation. *IEEE Transactions on Circuits and Systems II: Express Briefs*. 2023;70(4):1475-1479. doi: 10.1109/TCSII.2022.3221082

31. Xu B, Zhang L, Ji W. Improved Non-Singular Fast Terminal Sliding Mode Control With Disturbance Observer for PMSM Drives. *IEEE Transactions on Transportation Electrification*. 2021;7(4):2753-2762. doi: 10.1109/TTE.2021.3083925
32. Sun X, Cao J, Lei G, Guo Y, Zhu J. A Robust Deadbeat Predictive Controller With Delay Compensation Based on Composite Sliding-Mode Observer for PMSMs. *IEEE Transactions on Power Electronics*. 2021;36(9):10742-10752. doi: 10.1109/TPEL.2021.3063226
33. Van M, Kang HJ, Suh YS. A novel fuzzy second-order sliding mode observer-controller for a TS fuzzy system with an application for robot control. *Int. J. Precis. Eng. Manuf.*. 2013;14:1703–1711. doi: 10.1007/s12541-013-0229-1
34. Tsai CC, Wu HL. Nonsingular terminal sliding control using fuzzy wavelet networks for Mecanum wheeled omni-directional vehicles. In: IEEE. 2010:1–6
35. Yu D, Chen CLP, Xu H. Fuzzy Swarm Control Based on Sliding-Mode Strategy With Self-Organized Omnidirectional Mobile Robots System. *IEEE Transactions on Systems, Man, and Cybernetics: Systems*. 2022;52(4):2262-2274. doi: 10.1109/TSMC.2020.3048733

